Evaluation of synthetic routes to pigmentary grade bismuth vanadate

Elisabeth G. van der Linden, Luiz Fernando B. Malta*, Marta Eloisa Medeiros

Instituto de Quimica, Universidade Federal do Rio de Janeiro, Ilha do Fundão, 6th floor, 632, Cidade Universitaria, 21941-909 Rio de Janeiro, RJ, Brazil

ARTICLE INFO

ABSTRACT

Three methods of preparation of $BiVO_4$ were evaluated in order to select the most suitable to produce pigmentary grade material. Visible diffuse reflectance spectroscopy revealed that the pale appearance of the zircon structure phase of $BiVO_4$, produced *via* hydrothermal synthesis, was due to more selective absorption of UV radiation. On the other hand, the co-precipitated and oxide mixed $BiVO_4$, having a monoclinic scheelite structure, was characteristically yellow, but only the bright co-precipitated $BiVO_4$ was adequate for application as a pigment. X-Ray powder diffraction, differential thermogravimetry, Fourier-transform infrared spectroscopy and elemental analysis were employed to establish the source of such chromatic variation, while scanning electron microscopy established the source of the enhanced brightness for the $BiVO_4$ synthesized *via* the wet processes.

© 2010 Elsevier Ltd. All rights reserved.

1. Introduction

Bismuth vanadate, $BiVO_4$, was first synthesized by Roth and Waring in 1963 [1]. It presents polymorphism: the scheelite phase ($CaWO_4$) with a tetragonal unit cell ($I4_1/a$) has $a = b = 5.1507 \times 10^{-10}$ m and $c = 11.730 \times 10^{-10}$ m, and below 528 K transforms itself into a second phase of monoclinic crystalline system ($I2/b$) with $a = 5.1956 \times 10^{-10}$ m, $b = 11.7045 \times 10^{-10}$ m, $c = 5.0935 \times 10^{-10}$ m and $\delta = 90.383°$ [2]. A third phase has the zircon structure ($ZrSiO_4$) in a tetragonal unit cell ($I4_1/amd$) with $a = b = 7.3066 \times 10^{-10}$ m and $c = 6.4608 \times 10^{-10}$ m [3].

Vanadates are applicable as electric conductors [4–6], optical materials [7–9] and photocatalysts [10–15]. Specifically for $BiVO_4$, one of the most notable properties of $BiVO_4$ is thermochromism, evidenced by a color change from orange to dark red at 528 K. This phenomenon is associated with a second order ferroelastic transition in which the monoclinic-to-tetragonal transformation occurs with an increase in the strain in the crystalline lattice. In turn, this strain is a consequence of some atomic shifts in the monoclinic phase during the phase transition [10,16].

Many reports have attempted to produce $BiVO_4$ in the form of thin films [16–18], coatings and polycrystalline material [19] so as to generate yellow pigments [18,20]. Several procedures ranging from high temperature preparation, as in oxide mixing [1], to soft

synthesis, as in hydrothermal synthesis [3,21] and metalorganic decomposition [18] have been applied to obtain $BiVO_4$. However, we are not aware of any report in the literature comparing these methods in order to establish which is the most suitable to produce pigmentary grade $BiVO_4$.

The present manuscript introduces the syntheses of $BiVO_4$ through different methods in order to establish the most appropriate procedure to produce a pigmentary grade vanadate. Three preparation methods were evaluated, namely: oxide mixing, co-precipitation and hydrothermal synthesis. The color analysis was accomplished by using visible diffuse reflectance spectroscopy. To best understand how the synthetic route influences the color, pigment structure and chemical composition were monitored by using X-Ray powder diffraction (XRPD) differential thermogravimetry (DTA/TGA), Fourier-transform infrared spectroscopy (FTIR) and elemental analysis. In addition, the particle morphology of each pigment was visualized by using scanning electron microscopy (SEM).

2. Materials and methods

2.1. Materials and instrumentation

All reagents were purchased from Sigma–Aldrich, Riedel-de Haën and Vetec and used without further purification.

Visible Diffuse Reflectance Spectra were recorded on a Minolta CM − 3700 spectrometer. Samples were pressed in the form of

* Corresponding author. Tel.: +55 021 2562 7738; fax: +55 021 2562 7559.
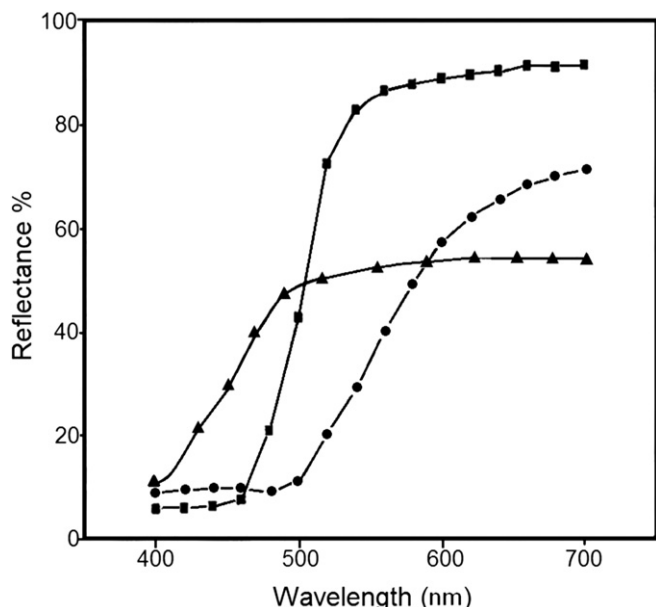E-mail addresses: lfbmalta@iq.ufrj.br, quimi1977@hotmail.com (L.F.B. Malta).

Fig. 1. Visible diffuse reflectance spectra of BiVO$_4$ synthesized *via* (●) oxide mixing, (■) co-precipitation and (▲) hydrothermal synthesis.

Table 1
CIELAB color parameters and band gap values of BiVO$_4$ synthesized by different methods.

Method	Color parameter					Band gap (Joule)
	L*	a*	b*	ΔE*	ΔL*	
Oxide mixing	66.05	24.23	49.31	—	—	3.25×10^{-19}
Co-precipitation	89.03	−3.98	85.26	51.15	22.98	3.70×10^{-19}
Hydrothermal synthesis	76.37	−5.08	20.27	42.53	10.32	4.08×10^{-19}

a disc. Measurements were performed using a BaSO$_4$ disc as a color standard. Color parameters were obtained using the Spectra Match 3.3 software (Minolta UK Ltd, Milton Keynes, UK). X-Ray powder diffraction analysis was performed using a Shimadzu XD-3A X-ray diffractometer, with CuKα radiation. The diffraction patterns were collected in the range of $10° \leq 2\theta \leq 60°$ with a 3.3×10^{-2} degrees per second scan. Cell parameters and crystalline systems were obtained employing DICVOL 91 software [22,23]. For visualizations by scanning electron microscopy a Jeol instrument, model JMS-T300 was used. Powders were dispersed on a flat sampler and they were doubly covered by graphite and gold vacuum depositions. A simultaneous DTA/TGA apparatus DTG-60 (Shimadzu) was used. Approximately 20 mg of each sample was weighted for analysis. Measurements were carried out under an argon atmosphere (8.3×10^{-7} m^3 s^{-1}) in the 298—873 K range with a 1.7×10^{-1} K s^{-1} rate. Fourier-transform infrared spectra were obtained in the 4000—400 cm^{-1} range by a Nicolet—Magna 760 spectrometer with a 4 cm^{-1} resolution. Samples were prepared using the KBr pellet technique. A 2400 CHN analyzer was used together with an AD-4 autobalance device, both from PerkinElmer.

2.2. Sample preparation

2.2.1. Oxide mixing method

BiVO$_4$ was obtained from oxide mixing of Bi$_2$O$_3$ (0.79 g, 1.7 mmol) and V$_2$O$_5$ (0.31 g, 1.7 mmol) in an agate mortar, using acetone to aid the homogenization process. Each solid mixture was left to stand at 373 K for 24 h, for the activation of precursors and then heated at 923 K in an aluminum crucible and quenched to room temperature after 14 h of reaction. For characterization the sample was used as produced.

2.2.2. Co-precipitation method

An orange gel was obtained after mixing 100 mL of alkaline solution (pH = 14) containing NaVO$_3$.H$_2$O (2.8 g, 20 mmol) and 100 mL of nitric solution (pH = 0) containing Bi(NO$_3$)$_3$.5H$_2$O (9.7 g, 20 mmol) at room temperature. The pH was adjusted to 3.5 and the suspension was vigorously mixed for 1 h. The solid was then filtered and washed with deionized water until a constant pH value

was reached. The solid material was placed in a platinum crucible and heated at 673 K for 1.5 h. For characterization the sample was used as produced.

2.2.3. Hydrothermal method

An orange/yellow precipitate was obtained after mixing 100 mL of alkaline solution (pH = 14) containing NaVO$_3$.H$_2$O (0.042 g, 0.3 mmol) and NaF (0.00012 g, 0.003 mmol) with 100 mL of nitric solution (pH = 0) containing Bi(NO$_3$)$_3$.5H$_2$O (0.14 g, 0.3 mmol). The pH was adjusted to 3.5 and the suspension was vigorously mixed for 1 h at room temperature. The suspension was then submitted to hydrothermal treatment at 363 K over 2 h during which time a pale yellow color developed. The reacted mixture was filtered and the powder was washed with sodium hydroxide solution (100 mL, 0.1 M) and dried at room temperature. For characterization the sample was used as produced.

3. Results and discussion

The visible diffuse reflectance spectra (Vis DR, Fig. 1) show inflection points at 550, 500 and 450 nm. Considering the absorption wavelength range of the co-precipitated BiVO$_4$ as the reference, these points indicate the red-shifted and blue-shifted
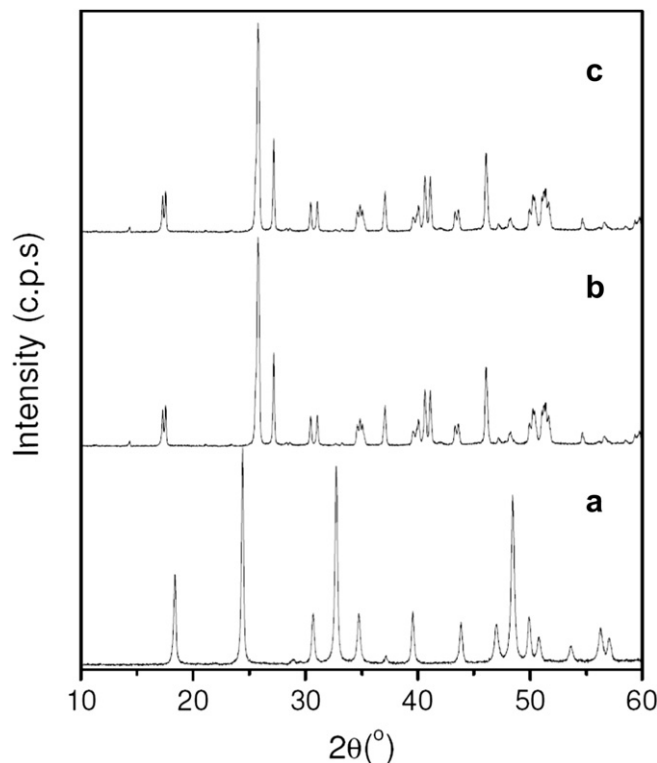

Fig. 2. Room-temperature X-rays powder diffraction profiles of BiVO$_4$ synthesized *via* (a) hydrothermal synthesis, (b) co-precipitation and (c) oxide mixing.

Table 2
Cell parameters of BiVO$_4$ synthesized by different methods, obtained using DICVOL 91 program [22,23].

Method	Cell parameter				
	a(10^{-10} m)	b(10^{-10} m)	c(10^{-10} m)	β(°)	V(10^{-30} m^3)
Oxide mixing	5.190 ± (0.002)	11.663 ± (0.006)	5.079 ± (0.002)	90.31 ± (0.04)	301.31
Co-precipitation	5.197 ± (0.002)	11.686 ± (0.004)	5.100 ± (0.002)	90.32 ± (0.03)	309.69
Hydrothermal synthesis	7.3036 ± (0.0007)	7.3036 ± (0.0007)	6.449 ± (0.001)	90	344.01

absorption maxima for the oxide mixed and hydrothermally synthesized compounds, respectively. This absorption is commonly assigned to the transition corresponding to the metal-to-ligand charge transfer (Bi^{3+} → VO$_4^{3-}$) [24].

From the DR spectra, the color parameters were obtained using the Spectra Match 3.3 software and were evaluated according to the CIELAB system. A brief discussion follows.

The color space L*a*b* (CIELAB System) [25] is one of the most used systems for color measurement. In this system, L* is the brightness and a* and b*are the chromaticity coordinates. The red, green, yellow and blue colors correspond to +a*, −a*, +b* and −b*, respectively. Each chromaticity coordinate ranges from zero (which corresponds to the achromatic center of the coordinate system) to 100. The brightness is obtained from this coordinate system. The color difference, ΔE, between a standard and the object to be measured is given by the following expression:

$$\Delta E = \left((\Delta L^*)^2 + (\Delta a^*)^2 + (\Delta b^*)^2\right)^{1/2}$$

in which ΔL*, Δa* and Δb* are the respective brightness and chromaticity differences. Table 1 shows the values of L*a*b*, obtained from the DR spectra using the Spectra Match 3.3 software. Delta-values were calculated using oxide mixed BiVO$_4$ as the standard.

Both co-precipitated and hydrothermally synthesized compounds are brighter than the standard, as observed by their ΔL* values. The lowest values of chromaticity for hydrothermally synthesized BiVO$_4$ are characteristic of its pale appearance, due to its maximum absorption in the UV region (Fig. 1). On the other hand, b* values greater than 50 are characteristic for yellow materials, which is the case of oxide mixed and co-precipitated compounds. The co-precipitation approach also led to low a* chromaticity which means that the yellow color is predominant for the corresponding BiVO$_4$. The conclusion is that pigmentary grade BiVO$_4$ was obtained solely when the co-precipitation method was used. The compound prepared by the oxide mixing method, though yellow, exhibits the lowest brightness among the compounds tested. It is thereby unsuitable for pigment application.

In the search to obtain the source of b* variation among our samples, characterization by X-Ray powder diffraction (XRPD) was employed. The XRPD profiles of the co-precipitated and oxide mixed vanadates (Fig. 2b and c) are assigned to the scheelite phase with a monoclinic system (see the indexation results, Table 2), while that corresponding to the hydrothermally synthesized BiVO$_4$ is characteristic of the zircon structure (Fig. 2a and Table 2). Both structures are described as having a Bi^{3+} cation 8-fold coordinated by VO$_4^{3-}$. [26] The same units of BiVO$_4$ per cell apply for both forms (Z = 4) [27]. However the values of the unit cell volume (Table 2), are distinct and thereby give rise to different packing of Bi^{3+} and VO$_4^{3-}$ centers. So it is possible to infer that as a consequence of its largest cell volume, the hydrothermally synthesized BiVO$_4$ should present lengthened mean bond distances, hence a shortened band width and an enlarged band gap [28]. This is confirmed by the band gap magnitudes obtained from DR spectra of Fig. 1 (see Table 1).

However color is not solely explained in terms of long-range structure. Chemical contamination by precursors and powder morphology also account for the source of color variation among these vanadates.

To detect any thermal events and/or mass losses associated with the heating of these materials showing the presence of non-expected chemical species in the pigment structure, DTA and TGA curves were collected (Fig. 3).

Thermal events were not observed for the oxide mixed BiVO$_4$. Even the transition of phase at 528 K was not detected although the room-temperature diffraction profile of this BiVO$_4$ was indexed as that of a monoclinic scheelite (see Table 2). While no mention concerning this phenomenon is found in the literature, it is our belief that a singular morphology and/or particle size of this powder may have influenced its thermal behavior [29]. In addition, not even the expected endothermic peak corresponding to its melting between 773 and 873 K was detectable. However, it was experimentally observed by us that this oxide mixed BiVO$_4$ melts above 1273 K therefore suggesting that the ferroelastic transition is also dislocated to higher temperatures.

Fig. 3a and b presents the TGA curves of hydrothermally synthesized and co-precipitated BiVO$_4$ displaying mass losses of 2.6% in the interval of 473–723 K; and of 2.7% in the interval of 713–852 K, respectively. The DTA curve of Fig. 3c allows identification of a sequence of endothermic and exothermic events at 573,
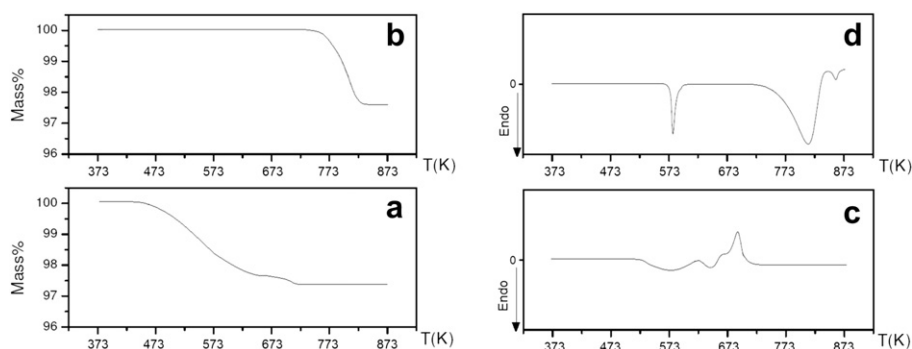

Fig. 3. TGA (a,b) and DTA (c,d) curves in the interval of 373–873 K of BiVO$_4$ synthesized via (a,c) hydrothermal synthesis and (b,d) co-precipitation. Analyses were carried out under an argon atmosphere (8.3 × 10^{-7} m^3 s^{-1}) with a heating rate of 1.7 × 10^{-1} K s^{-1}.
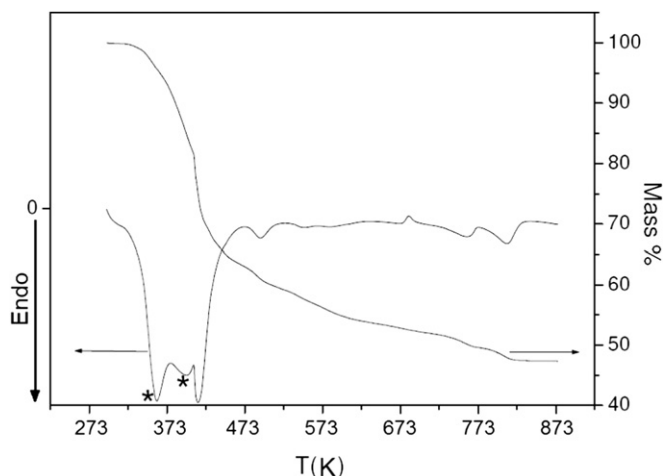
Fig. 4. TGA and DTA curves in the interval of 298—873 K of $Bi(NO_3)_3.5H_2O$. DTA peaks relative to water loss are highlighted. Analyses were carried out under an argon atmosphere (8.3×10^{-7} m^3 s^{-1}) with a heating rate of 1.7×10^{-1} K s^{-1}.

644 and 692 K which accompany the mass loss (Fig. 3a); by contrast, the curve of co-precipitated BiVO$_4$ (Fig. 3d) displays the transition from monoclinic to tetragonal at 576 K as well as that of an endothermic peak at 811 K correspondent to the mass loss event. Considering the thermal behavior of bismuth vanadates [5,6], no significant decomposition of its own structure should be expected; however, other chemicals, e.g. resulting from the reagents or degradation products thereof, can decompose with heating giving the profiles seen in Fig. 3a and b.

To investigate the validity of this residual reagent decomposition hypothesis, the DTG analysis of pentahydrated bismuth nitrate, Bi(NO$_3$)$_3$·5H$_2$O (Fig. 4) was carried out, since it is the precursor to both BiVO$_4$ pigments synthesized under mild conditions. The TGA data indicates that the water content of this salt (18.7%) is lost in the interval between room temperature and 407 K, correspondent to the two endothermic events in the DTA curve at 359 and 396 K (Fig. 4). Therefore the events at temperatures higher than 407 K are related to the decomposition process of the nitrate part of the bismuth salt. The TGA curve of the hydrothermally synthesized BiVO$_4$ displays a mass loss above 473 K, Fig. 3a, which, by analogy, could be assigned

as the decomposition of the nitrate ion residue from the Bi(NO$_3$)$_3$ precursor. Nevertheless, this loss can also be featured by the presence of structural water. The room-temperature FTIR spectrum of this vanadate was acquired in order to successfully prove the presence of NO$_3$ groups by detecting the stretching mode at 1394 cm^{-1} (see Supplementary material). The OH groups are also detectable by observing the stretching mode of O—H bonds at 3400 cm^{-1} and the bending mode of water at 1630 cm^{-1}; however the presence of these bands do not ensure the differentiation of loosely bound from structural water. The conclusion is that both nitrate and water are present in the hydrothermally synthesized sample.

Based on this previous discussion and according to the literature [3], there is evidence to affirm that NO$_3^-$ binds to Bi^{3+} through partial replacement of VO$_4^{3-}$. This phenomenon accounts for the pale appearance of the hydrothermally synthesized BiVO$_4$.

Concerning the co-precipitated compound, an endothermic event relative to a mass loss of 2.7% at 811 K is observed in its DTA/TGA curves (Fig. 3b and d). The same event is detected in the DTA/TGA curves of bismuth nitrate at 810 K (Fig. 4). Heating at 673 K is needed to form this BiVO$_4$ (see Materials and Methods section) hence explaining why mass losses at temperatures lower than 673 K are not detected (Fig. 3b and d). FTIR analysis of co-precipitated BiVO$_4$ (see Supplementary material) was not able to detect any trace of structural water and/or nitrate whose decomposition would afford the endothermic peak at 811 K. In order to further investigate this feature we proceeded to the elemental analysis, which gave 0.75% w/w of nitrogen. Considering that NO$_2$ was the gas that evolved during decomposition, this amount of nitrogen would be relative to a mass loss of 2.5%, close to that obtained from the TGA curve (2.7%, Fig. 3b). The hypothesis is that some crystallites of bismuth nitrate persisted as inner cores of the vanadate particles, thus only being decomposed at 811 K, above the temperature of calcination, 673 K. This hypothesis is validated by the fact that the low penetrating power of IR radiation does not allow the detection of occluded nitrate species by FTIR spectroscopy. Such phenomenon of occlusion should not influence the characteristic yellow color, an assumption that is corroborated by our previous analysis of color evidencing the pigmentary grade of this BiVO$_4$.

Powder morphology is another important characteristic to probe when focusing on color properties. For example, the surface of a particle with a fibrous texture tends to be associated with
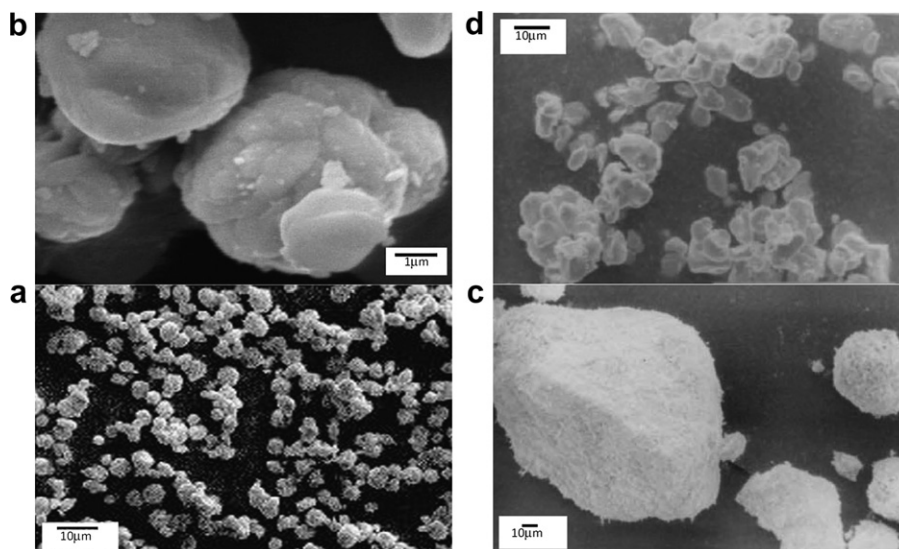

Fig. 5. SEM images of BiVO$_4$ synthesized via (a,b) hydrothermal synthesis (c) co-precipitation and (d) oxide mixing.

a radiating, brilliant $BiVO_4$ pigment [3]. This is the case in both the hydrothermally synthesized (Fig. 5a and b) and the co-precipitated compounds (Fig. 5c). On the other hand, the oxide mixed $BiVO_4$ is constituted of agglomerates with smooth surfaces (Fig. 5d). These results evidence how the particle morphology influences the L^* parameter, since the hydrothermally synthesized and co-precipitated compounds show enhanced brightness when compared with the oxide mixed $BiVO_4$ (see Table 1).

Concerning the correlation between powder morphology and chromaticity we see that while the pale hydrothermally synthesized $BiVO_4$ is constituted of monodispersed particles having $1-5$ μm (Fig. 5a), both yellow pigments, i.e., the co-precipitated and oxide mixed compounds, are constituted of a few irregular agglomerates with dimensions above 5 μm (Fig. 5c and d). In light scattering, the intensity of scattering is inversely proportional to the wavelength and directly proportional to the number of particles [30]. Since the hydrothermally synthesized particles are in greater amount than those in co-precipitated and oxide mixed samples, due to less agglomeration, these particles scatter more intensely the blue radiation, which is relative to the region of visible spectrum in which the absorption of light by $BiVO_4$ pigments is maximum. Therefore, higher reflectance in the blue region should be expected for the hydrothermally synthesized compound when compared with the other pigments, a hypothesis that is corroborated by the diffuse reflectance analysis in Fig. 1.

4. Conclusion

The discussion of the results has shed some light on the source of color variation among $BiVO_4$ compounds synthesized using different procedures. The chromaticity is influenced by the kind of crystalline structure of the pigment and by the presence of contaminant nitrate ions in its structure, partially replacing the VO_4^{3-} ions. This "anionic doping" by nitrate ions was observed only when the hydrothermal synthesis approach was applied, since for the co-precipitation procedure bismuth nitrate occlusion was suggested to have happened. Here, it is important to differentiate the hydrothermal synthesis from the co-precipitation method: the former is mainly based on continuously dissolving and precipitating particles favoring the nitrate doping, while the latter is constituted of a sudden co-precipitation, forming particles that can carry cores of $Bi(NO_3)_3$ resistant to heating until 723 K.

The SEM visualization has shown that brightness is enhanced in particles with rough and fibrous surfaces obtained using the soft synthesis methods. In pigment morphology, the mechanism through which the irregularly distributed agglomerates can change the light—pigment interaction from that of smaller monodisperse particles requires further investigation in the specialized literature.

AppendixSupplementary material

Supplementary material related to this article can be found at doi:10.1016/j.dyepig.2010.11.011.

References

[1] Roth RS, Waring JL. American Mineralogist 1963;48:p.1348.
[2] Sleight AW, H-Chen Y, Ferrati A, Cox DE. Materials Research Bulletin 1979; 14:1571.
[3] Wood P, Glasser FP. Ceramica International 2004;30:875.
[4] Stoltzfus MW, Woodward PM, Seshadri R, J-Klepeis H, Bursten B. Inorganic Chemistry 2007;46:3839.
[5] Malta LFB, Medeiros ME. Journal of Thermal Analysis and Calorimetry 2005; 81:149.
[6] Malta LFB, Medeiros ME. Journal of Thermal Analysis and Calorimetry 2007;87:883.
[7] Wadhawan VK. Phase Transitions 1982;3:3.
[8] David WIF, Glazer AM, Hewat AW. Phase Transitions 1979;1:155.
[9] J-Li F, Viehland D, Bhalla AS, Cross LE. Journal of Applied Physics 1992; 71:2106.
[10] Guo Y, Yang X, Ma F, Li K, Xu L, Yuan X, et al. Applied Surface Science 2010;256:2215.
[11] Zhou Y, Vuille K, Heel A, Probst B, Kontic R, Patzke GR. Applied Catalysis. A, General 2010;375:140.
[12] Li L, Yan B. Journal of Alloys and Compounds 2009;476:624.
[13] Liu W, Cao L, Su G, Liu H, Wang X, Zhang L. Ultrasonics Sonochemistry 2010; 17:669.
[14] Dunkle SS, Helmich RJ, Suslick KS. Journal of Physical Chemistry C 2009; 113:11980.
[15] Li H, Liu G, Duan X. Materials Chemistry and Physics 2009;115:9.
[16] Kumari N, Krupanidhi SB, Varma KBB. Materials Science and Engineering B 2006;138:22.
[17] Sayama K, Nomura A, Arai T, Sugita T, Abe R, Yanagida M, et al. Journal of Physical Chemistry B 2006;23:11352.
[18] Galembeck A, Alves OL. Thin Solid Films 2000;365:90.
[19] Rao CNR, Gopalakrishuam J. Accounts of Chemical Research 1987;20:228.
[20] Neves MC, Lehocky M, Soares R, Lapcik Jr L, Trindade T. Dyes and Pigments 2003;59:181.
[21] Liu JB, Wang H, Wang S, Yan H. Materials Science and Engineering:B 2003; 104:36.
[22] Louër PD. DICVOL 91, Laboratoire de Cristallochimie, Universite de Rennes, France, 1992.
[23] Boultif A, Louër PD. Journal of Applied Physics 1991;24:987.
[24] Ghamri J, Baussart H, Le Bras M, Leroy JM. Journal of Physics and Chemistry of Solids 1989;50:1237.
[25] Tücks A, Beck HP. Dyes and Pigments 2007;72:163.
[26] Nyman H, Hyde BG, Andersson S. Acta Crystallographica 1984;B40:441.
[27] Robinson K, Gibbs GV, Ribbe PH. American Mineralogist 1971;56:782.
[28] Smart L, Moore E. Solid state chemistry-an introduction. 2nd ed. Cleveland: CRC Press; 1995.
[29] Vallet P. Thermogravimétrie. Paris: Gauthier-Villars éditeur; 1972.
[30] Kennard TG, Howell DH. American Mineralogist 1941;26:405.